JOURNAL OF THERMOPHYSICS AND HEAT TRANSFER
Vol. 11, No. 3, July–September 1997

Natural Convection from Horizontal Circular and Square Toroids and Equivalent Cylinders

M. M. Yovanovich* and J. R. Culham†
University of Waterloo, Waterloo, Ontario N2L 3G1, Canada
and
S. Lee‡
Aavid Thermal Technologies, Inc., Laconia, New Hampshire 03247

General models are proposed for natural convection from horizontal circular and square isothermal toroids. The models consist of the linear superposition of the corresponding diffusive limits (shape factors) and the laminar boundary-layer asymptotes. The asymptote for the dimensionless shape factor for the circular toroid is used to find simple expressions for accurate calculation of the diffusive limits for the circular and square toroids over the full range of the outer-to-inner diameter ratios. Simple expressions are developed for accurate evaluation of the body–gravity function of the boundary-layer asymptote for the circular and square toroids by the method of inscribing and circumscribing circular cylinders and circular toroids within the equivalent square cylinder or square toroid. The Nusselt and Rayleigh numbers, and the dimensionless shape factor and body–gravity function are based on the characteristic body length, the square root of the total surface area of the body. The proposed models are compared against air data obtained for the circular and square toroids and equivalent cylinders. The agreement between theory and experiment is very good.

Nomenclature

A = surface area of the body, m^2
$\sqrt{A}$ = characteristic length of the body, m
$\tilde{A}$ = area fraction
$\tilde{A}_i$ = area fraction of the ith component
C_{CT}, C_{ST} = circular and square toroid body–gravity function coefficients
C^{∞}_{CT}, C^{∞}_{ST} = circular and square toroid shape factor coefficients
D = mean diameter of circular toroid, $(D_o + D_i)/2$, m
D_i, D_o = inner and outer diameters of toroid, m
d = ring or cylinder diameter, $(D_o - D_i)/2$, m
$F(Pr)$ = Prandtl number function,[12] $\equiv 0.670/[1 + (0.50/Pr)^{9/16}]^{4/9}$
$G_{\sqrt{A}}$ = laminar boundary-layer body–gravity function based on $\sqrt{A}$
$Gr_{\sqrt{A}}$ = Grashof number, $\equiv g\beta(T_s - T_a)(\sqrt{A})^3/\nu^2$
g = scalar gravitational acceleration, m/s^2
H = cuboid height, m
h = heat transfer coefficient, W/(m^2 K)
k = thermal conductivity, W/(m K)
L = cylinder or cuboid length, m
$Nu_{\sqrt{A}}$ = Nusselt number, $\equiv h\sqrt{A}/k$
$Nu^{\infty}_{\sqrt{A}}$ = diffusive limit, $Nu^{\infty}_{\sqrt{A}} = S^*_{\sqrt{A}}$
P_i, P_o = inner and outer perimeter of circular toroid, m
$P_{n-1/2}(\cdot)$ = toroidal or ring function of the first kind
Pr = Prandtl number, ν/α
$P(\theta)$ = local perimeter, m
Q = natural convection heat flow rate, W
$Q_{n-1/2}(\cdot)$ = toroidal or ring function of the second kind
Q_r = radiation heat flow rate, W
Q_{total} = total heat dissipation rate, W
$Ra_{\sqrt{A}}$ = Rayleigh number, $Gr_{\sqrt{A}}Pr$
S = side of square cylinder or square toroid, m
$S^*_{\sqrt{A}}$ = dimensionless shape factor
sq tor = square toroid
T_a = ambient temperature, K
T_s = surface temperature, K
W = cuboid width, m
α = thermal diffusivity, $\equiv k/\rho c_p$, m^2/s
β = volumetric expansion coefficient, K^{-1}
ε = emissivity
θ = angle between gravity vector and outward normal to surface, rad
ν = kinematic viscosity, $\equiv \mu/\rho$, m^2/s
ρ = density, kg/m^3
σ = Stefan–Boltzmann constant, 5.67×10^{-8} W/(m^2 K^4)

Subscript
$\sqrt{A}$ = based on $\sqrt{A}$, as the characteristic length

Superscript
∞ = estimated at $Ra \to 0$

Received April 15, 1996; presented as Paper 96-1838 at the AIAA 31st Thermophysics Conference, New Orleans, LA, June 17–20, 1996; revision received Jan. 17, 1997; accepted for publication Jan. 17, 1997.

*Professor and Director, Microelectronics Heat Transfer Laboratory, Department of Mechanical Engineering. Fellow AIAA.

†Research Associate Professor and Assistant Director, Microelectronics Heat Transfer Laboratory, Department of Mechanical Engineering.

‡Director, Advanced Thermal Engineering. Member AIAA.

Introduction

NATURAL convective cooling of certain electronic equipment requires correlation equations for predicting heat transfer from horizontal square toroids. A search of the heat transfer literature did not reveal any information about the natural convection heat transfer characteristics of horizontal square and circular toroids (see Fig. 1), which are also characterized by their inner and outer diameters and frequently by the ring diameter $d = (D_o - D_i)/2$ and the mean diameter $D = (D_o + D_i)/2$. Aihara and Saito[1] measured the free convective

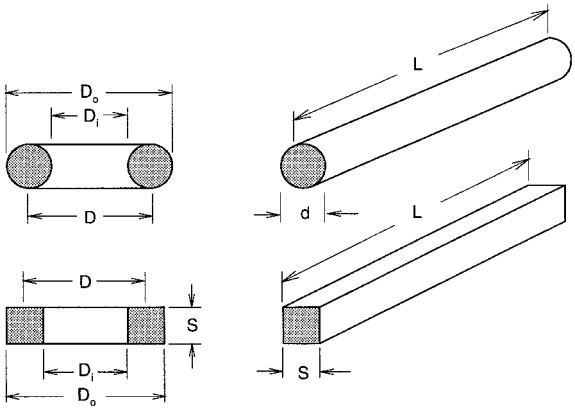

Fig. 1 Pertinent dimensions for circular and square toroids and cylinders.

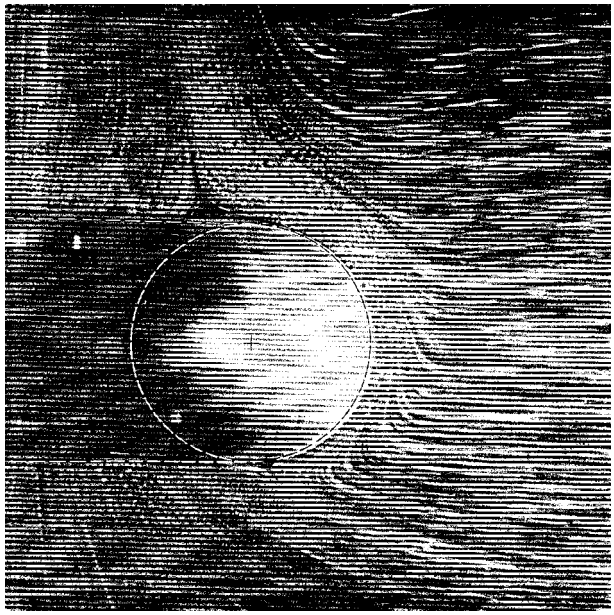

Fig. 2 Flow visualization for a circular toroid.[2]

velocity field and flow patterns around the periphery of horizontal circular toroids and compared their results with velocity measurements around the periphery of horizontal circular cylinders. The flow patterns are similar to that shown in Fig. 2 for a toroid with $D/d = 2$ at $Gr_d \equiv 10^5$. Aihara[2] did not, however, report heat transfer results.

The objectives of this paper are the following:

1) Propose procedures for developing models to predict natural convection from horizontal, isothermal circular and square toroids and equivalent cylinders.

2) Obtain simple correlation equations for air cooling.

3) Compare the proposed models and correlation equations with some experimental data.

General Three-Dimensional Natural Convection Model

The general expression for natural convective heat transfer from three-dimensional isothermal bodies

$$Nu_{\sqrt{A}} = Nu^{\infty}_{\sqrt{A}} + F(Pr)G_{\sqrt{A}}Ra^{1/4}_{\sqrt{A}} \tag{1}$$

was first proposed by Yovanovich.[3–5] This relationship is based on the linear superposition of the diffusive limit (shape factor) $Nu^{\infty}_{\sqrt{A}}$ corresponding to $Ra_{\sqrt{A}} \to 0$ and the thin laminar boundary-layer asymptote $F(Pr)G_{\sqrt{A}}Ra^{1/4}_{\sqrt{A}}$.

The laminar boundary-layer asymptote consists of the product of $F(Pr)$, $G_{\sqrt{A}}$, and $Ra_{\sqrt{A}}$. The characteristic length in the Nusselt and Rayleigh numbers and the body–gravity function is the square-root of the total active surface area $\sqrt{A}$, which was first proposed by Yovanovich[3–5] for natural and forced convection heat transfer from bodies of arbitrary shape. Yovanovich has previously used this characteristic length to nondimensionalize thermal constriction resistance[6–8] and conduction shape factors.[9–11]

The laminar Prandtl number function

$$F(Pr) = \frac{0.670}{[1 + (0.5/Pr)^{9/16}]^{4/9}} \tag{2}$$

was recommended by Churchill and Churchill[12] as the approximate universal function valid for all geometries and all values of the Prandtl number.

The body–gravity function

$$G_{\sqrt{A}} = \left\{ \frac{1}{A} \int \int_A \left[\frac{P(\boldsymbol{\theta})}{\sqrt{A}} \sin \theta \right]^{1/3} dA \right\}^{3/4} \tag{3}$$

was proposed by Lee et al.[13] for axisymmetric and two-dimensional geometries.

The proposed three-dimensional model, Eq. (1) has been experimentally validated[14] for a range of body shapes such as 1) axisymmetric spheroids (oblate and prolate), sphere; 2) elliptic and circular cylinders; 3) thin circular and square plates in the vertical and horizontal orientation; and 4) other body shapes (cube, cones with apex facing upward and downward).

Buoyancy-induced flow over complex body shapes can be modeled by 1) partitioning the total body surface into component surfaces corresponding to the fluid flow and 2) using the general formula, Eq. (3), for each component surface A_i to find the corresponding component body–gravity function $G_{\sqrt{A_i}}$.

The overall body–gravity function for the total body surface is determined by combining the component surfaces A_i and their respective $G_{\sqrt{A_i}}$ into a composite value. Equation (3) can be used for all surfaces except horizontal surfaces ($\sin \theta = 0$). At present, semiempirical methods must be used to model buoyancy-induced flow over horizontal surfaces.[14,15]

There are two important flow patterns for which the composite or overall body–gravity function can be determined with relative ease. These are complex bodies such as a circular cylinder with hemispherical ends that is placed in a large extent of air in either the horizontal (axis perpendicular to the gravity vector) or vertical (axis parallel to the gravity vector) orientations.

In the first orientation the two ends and the horizontal surface are cooled by different flows of air, and the component surfaces are said to be in the parallel flow pattern. In the second orientation the component surfaces are cooled by the same fluid flow that starts at the lower stagnation point, flows over the lower hemispherical end, then over the vertical cylindrical surface, and finally over the top hemispherical end. In this case the component surfaces are said to be in the series flow pattern.

The previous method of partitioning a complex body shape into parallel or series flow patterns can be applied to many interesting natural convection problems. Some orientations such as inclined short cylinders with flat ends or hemispherical ends, or inclined cuboids are more difficult to model.

If the buoyancy-induced flow over a complex body shape can be partitioned into N component surfaces with $\tilde{A}_i$, where $\sum_{i=1}^{i=N} \tilde{A}_i = 1$, and the corresponding $G_{\sqrt{A_i}}$ can be determined, then the composite body–gravity function for the entire body

surface can be evaluated by means of either the parallel flow pattern formula[13]

$$G_{\sqrt{A}} = \sum_{i=1}^{N} G_{\sqrt{A_i}} \tilde{A}_i^{7/8} \tag{4}$$

or the series flow pattern formula

$$G_{\sqrt{A}} = \left(\sum_{i=1}^{N} G_{\sqrt{A_i}}^{4/3} \tilde{A}_i^{7/6} \right)^{3/4} \tag{5}$$

For two-dimensional surfaces, such as vertical disks or plates of arbitrary shape with variable perimeter $P(z)$, the body–gravity function can be easily obtained from the following simple formula, which was derived from Eq. (3) after setting $\sin \theta = 1$

$$G_{\sqrt{A}} = \frac{2}{A^{7/8}} \int_0^{P_{\max}/2} S(z)^{3/4}\, dz \tag{6}$$

where $S(z)$ denotes the flow distance from the leading edge to the trailing edge of the differential surface dz and $P_{\max}$ is the maximum perimeter of the surface.

These formulas along with the semiempirical results recommended by Yovanovich and Jafarpur[15] for horizontal surfaces facing upward or downward will be used to determine the composite body–gravity function for the horizontal circular and square toroids and their equivalent cylinders.

Diffusive Limits

Since $Nu^{\infty}_{\sqrt{A}}$ is identical to $S^{*}_{\sqrt{A}}$, (Ref. 3) analytical or numerical solutions for the circular and square toroids and their equivalent cylinders must be obtained.

Circular Toroid

Analytical and numerical solutions for isothermal circular toroids are available.[11,17–19] The dimensionless shape factor obtained from the analytical solution is

$$S^{*}_{\sqrt{A}} = \frac{4}{\pi} \sqrt{\frac{D}{d} - \frac{d}{D}} \left[\frac{Q_{-1/2}(D/d)}{P_{-1/2}(D/d)} + 2 \sum_{n=1}^{\infty} \frac{Q_{n-1/2}(D/d)}{P_{n-1/2}(D/d)} \right] \tag{7}$$

with $D/d \geq 1$. The special functions $P_{n-1/2}(D/d)$ and $Q_{n-1/2}(D/d)$ are called toroidal or ring functions. These functions can be calculated accurately by means of *Mathematica*,[20] and their properties are known.[18,21] The previous series solution converges very slowly as $D/d \to 1$; however, it converges rapidly to the asymptote for $D/d > 8$:

$$S^{*}_{\sqrt{A}} = 2\pi \frac{\sqrt{D/d}}{\ell n(8D/d)} \tag{8}$$

For $D/d = 1$, the value of $S^{*}_{\sqrt{A}}$ can be computed numerically with acceptable accuracy,[16] as

$$S^{*}_{\sqrt{A}} = \frac{8}{\pi} \int_0^{\infty} \frac{dt}{I_0^2(t)} = 3.4827 \tag{9}$$

where $I_0(t)$ is the modified Bessel function of the first kind of zero order.

Values of $S^{*}_{\sqrt{A}}$ for small and large values of D/d are given in Tables 1 and 2, respectively. The values of $S^{*}_{\sqrt{A}}$ in Table 1 can be approximated by the constant 3.449 with a maximum error less than 1%.

The asymptote for large values of D/d, given in Eq. (8), when multiplied by

$$C^{\infty}_{CT} = (81/80) + (e^{-D/d}/\sqrt{4.5}) \tag{10}$$

provides a means of estimating $S^{*}_{\sqrt{A}}$ in the range $2 \leq D/d < 10$. Table 2 compares the exact values of $S^{*}_{\sqrt{A}}$, obtained from Eq. (7) with values computed by means of the modified asymptote for $2 \leq D/d < 10$ and values calculated using the asymptote for $D/d \geq 10$. The maximum error is less than 0.7%.

Square Toroid

The square toroid shown in Fig. 1 does not have an analytical solution. Numerical results based on the surface element method (SEM) using ring sources[11,22] are available for a range of values of $2S/D_o$. For convenience and completeness, the SEM values of $S^{*}_{\sqrt{A}}$ are given in Table 3.

An accurate correlation equation for the square toroid results can be developed by transforming the square toroid into a similar circular toroid. This is accomplished by two simple geometric rules: 1) set the surface area of the similar circular toroid equal to that of the square toroid and 2) set the mean

Table 1 Dimensionless shape factor for small D/d

D/d	$S^{*}_{\sqrt{A}}$	D/d	$S^{*}_{\sqrt{A}}$
1.0	3.483	1.6	3.415
1.1	3.455	1.7	3.418
1.2	3.437	1.8	3.423
1.3	3.425	1.9	3.430
1.4	3.417	2.0	3.439
1.5	3.414	——	——

Table 2 Dimensionless shape factor for large D/d

D/d	$S^{*}_{\sqrt{A}}$ exact	$S^{*}_{\sqrt{A}}$ modified
2	3.439	3.449
3	3.570	3.548
4	3.728	3.703
5	3.885	3.868
6	4.036	4.030
7	4.179	4.183
8	4.314	4.327
9	4.442	4.463
10	4.564	4.534
20	5.548	5.537
30	6.286	6.279
40	6.893	6.889
50	7.418	7.415

Table 3 Dimensionless shape factor for square toroids

$2S/D_o$	$S^{*}_{\sqrt{A}}$ SEM	$S^{*}_{\sqrt{A}}$ approximate
0.9999	3.419	3.374
0.9	3.345	3.311
0.8	3.302	3.280
0.7	3.289	3.277
0.6	3.310	3.307
0.5	3.374	3.378
0.4	3.496	3.510
0.3	3.712	3.744
0.2	4.106	4.167
0.1	5.012	5.075
0.05	6.241	6.321
0.01	10.90	11.02
0.001	26.17	26.38
0.0001	66.64	67.07

perimeter of the similar circular toroid equal to that of the square toroid. Applying these rules gives the geometric relationship between the transfomed circular toroid and the square toroid as

$$\frac{D}{d} = \frac{\pi}{4}\left(\frac{D_o}{S} - 1\right) = \frac{\pi}{4}\frac{D}{S} \tag{11}$$

which provides good results when it is substituted into Eq. (8) for $2S/D_o \leq 0.1$.

To achieve good agreement with the SEM results for $2S/D_o > 0.1$, the correction

$$C_{ST}^{\infty} = (161/160) + (e^{-D/d}/\sqrt{18}) \tag{12}$$

is recommended, where the equivalent D/d is given by Eq. (11). These correlation equations provide values of $S^*_{\forall\sqrt{A}}$ for the square toroid over the full range of the parameter $2S/D_o$, and when compared with the SEM results the maximum difference is less than 0.8%.

Circular Cylinder

The dimensionless shape factor equation for circular cylinders of L and d

$$S^*_{\forall\sqrt{A}} = \frac{3.192 + 2.773(L/d)^{0.76}}{\sqrt{1 + 2(L/d)}} \qquad 0 \leq \frac{L}{d} \leq 8 \tag{13}$$

was recommended by Yovanovich[3] and

$$S^*_{\forall\sqrt{A}} = \frac{4\sqrt{L/d}}{\ell n(2L/d)} \qquad \frac{L}{d} > 8 \tag{14}$$

which is based on the long prolate spheroid asymptote.[3]

Square Cylinder

Analytical solutions for the square cylinder are not available. One can, however, estimate the values of $S^*_{\forall\sqrt{A}}$ by means of the process of inscribing and circumscribing circular cylinders inside and outside the square cylinder. This method provides two estimates of the length-to-diameter ratio: 1) L/S and 2) $L/(\sqrt{2}S)$. It is recommended that one take the geometric mean of these values, i.e., $L/(2^{1/4}S)$, to represent the effective aspect ratio of the similar circular cylinder. Inserting the recommended value of the aspect ratio [i.e., $L/d = L/(2^{1/4}S)$] into the equation for the circular cylinder [Eq. (13) or Eq. (14)] provides values of $S^*_{\forall\sqrt{A}}$, which agree well with reported numerical values obtained for square cylinders.

The previous equations for the dimensionless shape factor for circular and square toroids and circular and square cylinders will be used to develop general models for natural convective heat transfer from these bodies in a subsequent section.

Body-Gravity Functions for Toroids and Cylinders

The general expression for the body-gravity function with the parallel and series flow pattern composite equations[13] will be used to develop general equations for 1) horizontal circular cylinders with active ends, 2) horizontal square cylinders with active ends, 3) horizontal circular toroids, and 4) horizontal square toroids.

Circular Cylinder with Active Ends

The body-gravity function for the sides of a horizontal circular cylinder is $G_{\sqrt{A}} = 0.891(L/d)^{1/8}$, and it is $G_{\sqrt{A}} = 1.0209$ for each vertical circular end according to Lee et al.[13] By means of the composite formula [Eq. (4)], these relationships combine to

$$G_{\sqrt{A}} = 0.891\,\frac{(0.681 + L/d)}{(0.5 + L/d)^{7/8}} \qquad 0 \leq \frac{L}{d} < \infty \tag{15}$$

The constants in the numerator and denominator account for heat transfer through the two active ends.

Square Cylinder with Active Ends

The body-gravity function for horizontal square cylinders with active ends can be developed directly from the cuboid model of Yovanovich and Jafarpur[15]

$$G_{\sqrt{A}} = 2^{1/8}\left[\frac{0.625(L/S)^{4/3} + (1 + L/S)^{4/3}}{(1 + 2L/S)^{7/6}}\right]^{3/4} \qquad 0 \leq \frac{L}{S} < \infty \tag{16}$$

after putting $H = W = S$, where H and W represent the height and width, respectively, of the cuboid.

The body-gravity function can also be estimated by the method of inscribing and circumscribing a circular cylinder inside and outside the square cylinder. This approach gives two values of the effective length-to-diameter ratio: $D/d = L/S$ and $D/d = L/(\sqrt{2}S)$ for the inscribed and circumscribed cylinders, respectively. When these two values are substituted into Eq. (15), two estimates of $G_{\sqrt{A}}$ are obtained that are usually quite close.

Horizontal Circular Toroid

The toroid surface is partitioned into the outer and inner subsurfaces by passing a vertical plane through the ring axis. The geometric parameters for the outer and inner subsurfaces in terms of the toroid parameter $D/d > 1$ are as follows:

Local Perimeter and Differential Area:

$$P_{o,i} = (\pi/2)d[(D/d) \pm \sin\theta] \tag{17}$$

$$dA_{o,i} = \frac{\pi}{2}d^2\left(\frac{D}{d} \pm \sin\theta\right)d\theta \tag{18}$$

The positive and negative signs are appropriate for the outer and inner subsurfaces, respectively.

Area and Area Fraction:

$$A_{o,i} = (\pi/2)d^2[\pi(D/d) \pm 2] \tag{19}$$

$$\tilde{A}_{o,i} = \tfrac{1}{2} \pm 1/[\pi(D/d)] \tag{20}$$

Body-Gravity Function:

Integration of the general expression with the previous geometric parameters yields the body-gravity functions for the outer and inner subsurfaces

$$G_{o,i} = \left\{\frac{2\pi}{[\pi(D/d) \pm 2]^7}\right\}^{1/8}\left[\int_0^{\pi}\sin^{1/3}\theta\left(\frac{D}{d} \pm \sin\theta\right)^{4/3}d\theta\right]^{3/4} \tag{21}$$

Table 4 Values of body-gravity function for circular toroid and equivalent circular cylinder

D/d	G_o	G_i	G_{tor}	G_{cyl}	% difference
1.5	1.072	0.870	1.089	1.081	0.70
2.0	1.093	0.938	1.125	1.121	0.36
2.5	1.112	0.986	1.155	1.153	0.23
3.0	1.129	1.022	1.181	1.179	0.15
3.5	1.145	1.052	1.204	1.202	0.11
4.0	1.159	1.076	1.224	1.223	0.08
4.5	1.172	1.098	1.241	1.240	0.06
5.0	1.185	1.117	1.258	1.257	0.05

The overall body–gravity function for the toroid can be obtained by means of the composite expression

$$G_{\text{tor}} = G_o \tilde{A}_o^{7/8} + G_i \tilde{A}_i^{7/8} \tag{22}$$

Numerical integrations of Eq. (21) with Eq. (22) yield values of G_o, G_i, and G_{tor}, given in Table 4 for $1.5 \leq D/d \leq 5$.

Equivalent Circular Cylinder

The equivalent horizontal circular cylinder is defined to be a cylinder whose diameter is equal to the diameter of the toroid and whose length is $L = \pi D$. By means of Eq. (3) with appropriate geometric parameters ($P = 2L$, $\mathrm{d}A = Ld\,\mathrm{d}\boldsymbol{\theta}$, $A = \pi Ld$), one obtains

$$G_{\text{cyl}} = 2^{1/4}\left(\frac{1}{\pi}\int_0^{\pi} \sin^{1/3}\theta\,\mathrm{d}\theta\right)^{3/4}\left(\frac{D}{d}\right)^{1/8} = 1.028\left(\frac{D}{d}\right)^{1/8} \tag{23}$$

in terms of the toroid parameter D/d. Numerical values of G_{cyl} are presented in Table 4 along with the percent difference between G_{tor} and G_{cyl}. The values of the body–gravity function for the toroid are greater than the values for the equivalent cylinder; however, the percent difference is less then 0.7%.

The body–gravity function for the equivalent cylinder can be used to estimate the body–gravity function for all toroids ($D/d \geq 1.5$) with negligible error.

Horizontal Square Toroid

The body–gravity function for the horizontal square toroid cannot be developed in a simple direct manner because of its geometric complexity. It is, therefore, necessary to obtain approximate solutions using known solutions. This can be accomplished in two related ways:

1) By inscribing and circumscribing circular cylinders inside and outside the equivalent square cylinder of length $L = \pi D$, then using Eq. (23) for the body–gravity function of the equivalent circular cylinder with insulated ends, find two values of $G_{\sqrt{A}}$ that are expected to bound the value for the square toroid.

2) Inscribing and circumscribing circular toroids inside and outside the square toroid, then using the result obtained for the equivalent circular cylinder. This method of inscribing and circumscribing circular cylinders inside square cylinders has been used by Jafarpur[14] to find bounds on $G_{\sqrt{A}}$ that were observed to be close.

Since the two approaches just described lead to similar results, the second approach will be used here. The inscribed circular toroid parameter is

$$D/d = (D_i/S) + 1 = D/S \tag{24}$$

and for the circumscribed circular toroid the parameter is

$$\frac{D}{d} = \frac{1}{\sqrt{2}}\left(\frac{D_i}{S} + 1\right) = \frac{D}{\sqrt{2}S} \tag{25}$$

These relationships, after substitution into Eq. (23), give the general relationship for bounds on the body–gravity function for horizontal square toroids

$$0.984(D/S)^{1/8} < G_{\sqrt{A}}^{\text{sq tor}} < 1.028(D/S)^{1/8} \tag{26}$$

The maximum and minimum values of $G_{\sqrt{A}}$ differ by 4.4%, which supports the findings of Jafarpur[14] for other body shapes.

For the square toroid with $D/S = 3$, we find the body–gravity function to lie in the tight range

$$1.129 < G_{\sqrt{A}}^{\text{sq tor}} < 1.179 \tag{27}$$

The third more complex method of determining $G_{\sqrt{A}}$ is based on the partitioning of the square toroid surface into component surfaces. One approach is based on dividing the total surface into the inner and the outer portions that consist of the bottom, side, and top components. The inner and outer portions can be modeled as component surfaces that are in the series flow pattern similar to the approach taken for the circular toroid. This will give complex relationships for the body–gravity functions for the inner and outer portions. Finally, the overall body–gravity function can be determined by using the parallel flow pattern equation. When this method is applied to the square toroid with $D/S = 3$, one finds $G_{\sqrt{A}} = 1.1988$, which is 1.7% greater than the value obtained by inscribing a circular toroid inside the square toroid or inscribing a circular cylinder inside the equivalent square cylinder.

Models for Circular and Square Toroids

The shape factor and body–gravity function results presented in the preceding sections can be used to develop general models for natural convective heat transfer from horizontal circular and square toroids and their equivalent cylinders. The general expression for natural convective heat transfer for three-dimensional bodies, as given in Eq. (1), can be used in conjunction with the shape factors and body–gravity functions presented next, to obtain expressions for $Nu_{\sqrt{A}}$ for circular and square toroids and circular and square cylinders.

Circular Toroid:

$$Nu_{\sqrt{A}}^{\infty} = \begin{cases} 3.449 & \text{for } D/d < 2.0 \\ C_{\text{CT}}^{\infty} 2\pi \dfrac{(D/d)^{1/2}}{\ell n(8D/d)} & \text{where } C_{\text{CT}}^{\infty} = \begin{cases} \text{Eq. (10)} & \text{for } 2 \leq D/d < 10 \\ 1 & \text{for } D/d > 10 \end{cases} \end{cases}$$

$$G_{\sqrt{A}} = C_{\text{CT}}(D/d)^{1/8} \text{ with } 1.028 < C_{\text{CT}} < 1.121$$

Square Toroid:

$$Nu_{\sqrt{A}}^{\infty} = C_{\text{ST}}^{\infty}\pi^{3/2}\frac{(D/S)^{1/2}}{\ell n(2\pi D/S)} \text{ with } C_{\text{ST}}^{\infty} = \begin{cases} \text{Eq. (12)} & \text{for } 2S/D_o > 0.1 \\ 1 & \text{for } 2S/D_o \leq 0.1 \end{cases}$$

$$G_{\sqrt{A}} = C_{\text{ST}}(D/S)^{1/8} \text{ with } 0.984 < C_{\text{ST}} < 1.028$$

Circular Cylinder (Ends Active):

$$Nu^{\infty}_{\sqrt{A}} = \begin{cases} \dfrac{3.192 + 2.773(L/d)^{0.76}}{\sqrt{1 + 2(L/d)}} & \text{for } 0 \le L/d \le 8.0 \text{ [Eq. (13)]} \\ \dfrac{4\sqrt{L/d}}{\ell n(2L/d)} & \text{for } L/d > 8 \text{ [Eq. (14)]} \end{cases}$$

$$G_{\sqrt{A}} = 0.891 \frac{(0.681 + L/d)}{(0.5 + L/d)^{7/8}} \text{ for } 0 \le L/d < \infty \text{ [Eq. (15)]}$$

Square Cylinder (Ends Active):

$$Nu^{\infty}_{\sqrt{A}} = \text{same as circular cylinder with } L/d = L/(2^{1/4}S)$$

$$G_{\sqrt{A}} = 0.595 \frac{[0.625(L/S)^{4/3} + (1 + L/S)^{4/3}]^{3/4}}{(0.5 + L/S)^{7/8}} \text{ for } 0 \le L/S < \infty \text{ [Eq. (16)]}$$

Experiments and Results

Steady-state heat transfer measurements were made for the body shapes depicted in Fig. 1. The body dimensions are found in Table 5. All bodies had the same total surface area. Each body was machined from aluminum alloy 6061-T6 to a 0.1 mm tolerance, and then highly polished. The low emissivity of the polished surface minimized the radiation heat loss, and the high conductivity (201 W/mK) of the material produced a nearly isothermal surface temperature. The measurements for each case were obtained when the body was suspended in the central square section of the vertical wind tunnel whose cross-sectional dimensions are 300 by 300 mm. Each body was suspended in the test section using the lead wires of the embedded heater and thin low conductivity cotton filaments to level and support the bodies in a horizontal orientation. The surface temperature T_s was measured by three 5-mil copper–constantan thermocouples epoxied into 0.5-mm holes. Power was supplied to the body through a 95-Ω resistance heater that was cemented into a hole 7 mm in diameter by 45 mm deep. To minimize conduction losses from the body, the diameter of the copper heater leads and the thermocouple leads were made as small as possible. To ensure that the bodies were maintained isothermal, a high-conductivity aluminum-based thermal epoxy was used to attach all leads and thermocouples.

Three thermocouples located within the test section were used to measure the ambient temperature T_a.

The power to the resistance heaters ranged between 0.5–11 W in increments of 0.5 W. Steady state was achieved when the following three conditions had been satisfied. First, the temperature difference between two consecutive readings was less than 0.1°C, the percent difference between two consecutive temperature readings was less than 0.1%, and finally a minimum time of 20,000 s, based on the lumped-capacitance of the body, must be exceeded. When these conditions were achieved, the heater power and the thermocouple readings were determined based on the average of the next five consecutive readings. All tests were conducted with half the data obtained for heater power increasing from its lowest level to its highest, and the other half of the data were obtained for heater power decreasing from the high to low power levels. Typically about 22 sets of data were obtained for each body.

Table 5 Critical dimensions for body shapes tested

Shape	D, mm	d or S, mm	L, mm
Circular toroid	58.62	19.54	——
Square toroid	51.96	17.32	——
Circular cylinder	——	19.54	174.43
Square cylinder	——	17.32	154.58

The average surface temperature ranged between 30–120°C; and the average surface-to-ambient temperature drop ranged between 7–95°C. The thermophysical properties in the Nusselt and Rayleigh numbers were evaluated at the film temperature $(T_s + T_a)/2$. The volumetric coefficient of expansion was calculated at the ambient temperature. Property equations were developed[23] from the tabulated data of Hilsenrath et al.[24]

The Nusselt and Rayleigh numbers for all bodies were based on $\sqrt{A}$ = 106.3 mm. The Rayleigh number range was from 8×10^5 to 7×10^6 and the Nusselt number range was from 20 to 35.

The emissivity of each body was measured in a vacuum system. The emissivity-area product εA was determined for each body by means of

$$Q_r = \varepsilon A \sigma (T_s^4 - T_a^4) \tag{28}$$

where T_s is the average of three thermocouple measurements and T_a is the average of three thermocouples that were attached to the walls of the bell-jar or freely suspended near the bell-jar wall. The measured surface temperatures did not vary by more than 1.5% and the ambient temperature had a small variation of 0.9%. The power to the resistance heaters varied from 0.75 to 2.4 W in increments of 0.825 W to produce a surface temperature range of 95–190°C. The measured emissivity for each body ranged between 0.081–0.095.

The net heat transfer by natural convection Q was calculated as the difference between the total power supplied to the resistance heaters and the radiative heat loss plus lead losses [$Q = Q_{\text{total}} - (Q_r + Q_{\text{leads}})$].

Conduction losses from each body along the heater leads were calculated as $0.0024(T_s - T_a)$, whereas the losses from the thermocouple leads were calculated as $0.00041(T_s - T_a)$ $\times$ number of thermocouples attached to the body. All conduction lead losses were based on conduction through a rod with a diameter and thermal conductivity equivalent to the leads.

Comparison of Models and Air Data

The proposed general models for natural convection from isothermal circular and square toroids and equivalent cylinders will be compared against air data (Pr = 0.71) for which the Prandtl number function $F(Pr)$ = 0.513.

Circular and Square Cylinders

The air data of Clemes[25] for a circular cylinder with L/d = 10.24 and a square cylinder with L/S = 10.13 are used to

validate the proposed cylinder models that reduce to the following correlation equations:

$$Nu_{\sqrt{A}} = 4.24 + \begin{bmatrix} 0.682 \\ 0.625 \end{bmatrix} Ra_{\sqrt{A}}^{1/4} \tag{29}$$

for the circular cylinder and

$$Nu_{\sqrt{A}} = 4.12 + \begin{bmatrix} 0.625 \\ 0.603 \end{bmatrix} Ra_{\sqrt{A}}^{1/4} \tag{30}$$

for the square cylinder. The two values before the Rayleigh number represent the upper and lower values of the body–gravity function multiplied by the Prandtl number function.

The correlation equations and the data of Clemes[25] are compared in Fig. 3. The agreement between the correlation equations (which differ by less than 9%), for the circular cylinder and the circular and square cylinder data is excellent over five-to-six decades of the Rayleigh number. The very close agreement of the data for the circular and square cylinders also confirms the proposed method of inscribing and circumscribing circular cylinders within and outside square cylinders to obtain estimates of the body–gravity function.

The equivalent circular cylinder $L/d = 8.93$ used in this research has the correlation equation

$$Nu_{\sqrt{A}} = 4.15 + \begin{bmatrix} 0.673 \\ 0.617 \end{bmatrix} Ra_{\sqrt{A}}^{1/4} \tag{31}$$

and the equivalent square cylinder $L/S = 8.92$ has the correlation equation

$$Nu_{\sqrt{A}} = 4.05 + \begin{bmatrix} 0.617 \\ 0.596 \end{bmatrix} Ra_{\sqrt{A}}^{1/4} \tag{32}$$

The circular cylinder data of Clemes[25] and the present data are compared with the model predictions in Fig. 4. The two sets of data are in excellent agreement with each other and they lie between the bounds that differ by less than 9% at the higher values of Rayleigh number. The data are very close to the lower bound established for the $L/d = 10.24$ cylinder.

Circular and Square Toroids

The correlation equations for the circular and square toroids in the present investigation, with $D/d = 3.0$, are based on the exact solution value and the numerical value, respectively, for the shape factor, and the upper and lower values of the body–gravity functions as discussed in previous sections on the body–gravity function.

The circular toroid equation reduces to

$$Nu_{\sqrt{A}} = 3.57 + \begin{bmatrix} 0.660 \\ 0.605 \end{bmatrix} Ra_{\sqrt{A}}^{1/4} \tag{33}$$

and for the square toroid the equation becomes

$$Nu_{\sqrt{A}} = 3.37 + \begin{bmatrix} 0.605 \\ 0.579 \end{bmatrix} Ra_{\sqrt{A}}^{1/4} \tag{34}$$

The circular toroid data and the corresponding predictions are compared in Fig. 5. The agreement between the upper bound equation and the data is excellent. The lower bound predictions lie approximately 9% below the data.

The square toroid data and the model predictions that differ by less than 4.5% are also compared in Fig. 5. The data lie very close to the lower bound curve at the lower values of Rayleigh number and fall between the two curves at the higher values of Rayleigh number.

The comparisons shown in Figs. 3–5 confirm the validity of the correlation equations that come from the general equations developed in this work. The general equations were based on the general two-term model proposed by Yovanovich[3–5] for natural convection heat transfer from three-dimensional, convex, isothermal bodies of arbitrary shape.

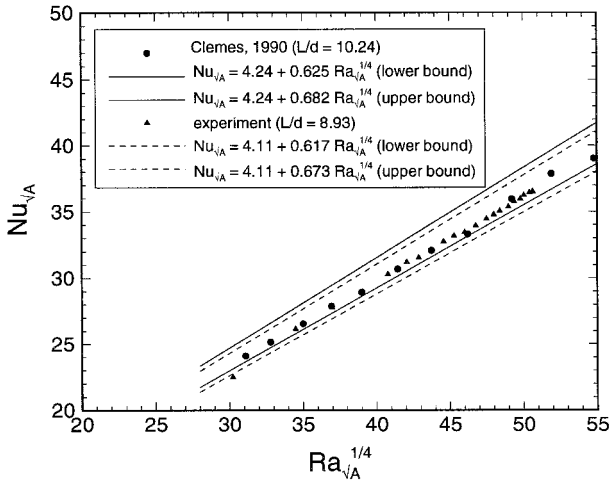

Fig. 4 Comparison of circular cylinder experimental data with bounding solutions for $L/d = 10.24$ and 8.93.

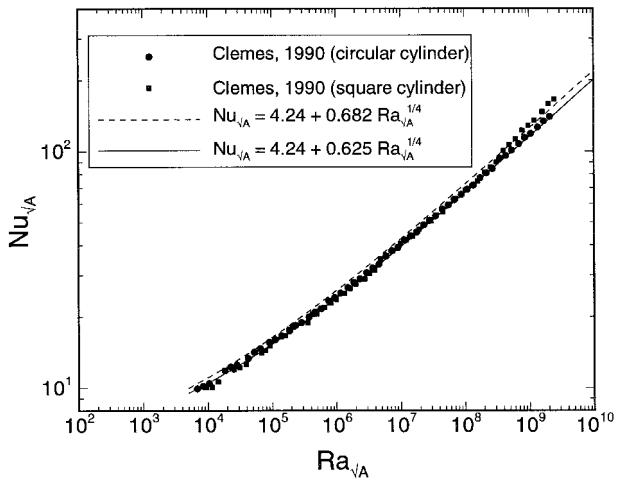

Fig. 3 Comparison of experimental data[25] with correlation equations for circular and square cylinders.

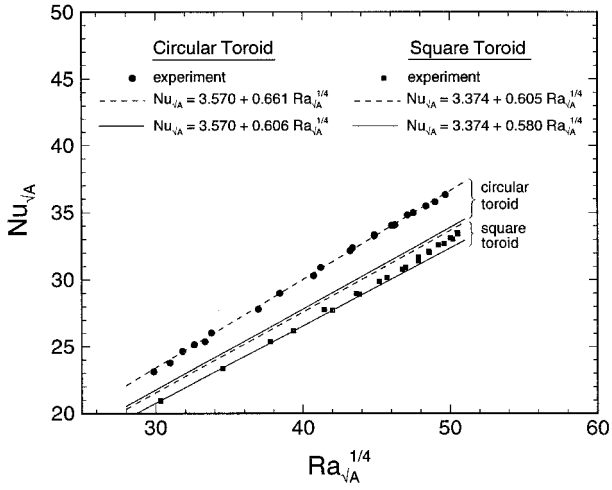

Fig. 5 Comparison of experimental data and prediction for a circular and square toroid.

It should be noted that the lower and upper bound values in Eqs. (29), (31), and (33) were calculated based on $F(Pr)G_{\sqrt{A}}$ with $Pr = 0.71$, where the upper bound is a factor of $2^{1/8}$ larger than the lower bound. The effect of this factor is seen in Figs. 4 and 5.

Summary and Conclusions

General models for natural convection from horizontal isothermal circular and square toroids and their equivalent cylinders have been presented. Simple relationships are proposed for accurate calculation of the diffusive limits (shape factors) for the circular and square toroids for a wide range of their outer-to-inner diameter ratios. Methods and relationships are presented for the evaluation of the body–gravity functions for the circular and square toroids and their equivalent cylinders. The numerical values of the body–gravity function are found to lie in relatively narrow ranges for both circular and square toroids.

Results from an experimental program are also presented. The air data are found to be in very good agreement with the proposed models and their corresponding correlation equations. The circular toroid data agree well with the upper bound model and the square toroid data lie between the bounds established by the models based on the inscribed and circumscribed method. The difference between these two models is approximately 4.4%, and the data were in excellent agreement with the mean values of the two models.

The data from the equivalent circular and square cylinders were in very good agreement with the proposed models.

Acknowledgments

The authors acknowledge the financial support of the Natural Sciences and Engineering Research Council of Canada and Bell-Northern Research of Kanata. We also acknowledge the many useful discussions with K. Jafarpur concerning the modeling of the horizontal square toroid. We thank Sorin Witzman of Bell-Northern Research for bringing the problem to our attention.

References

[1]Aihara, T., and Saito, E., "Measurements of Free Convection Velocity Field Around the Periphery of a Horizontal Torus," *Journal of Heat Transfer*, Vol. 94, No. 1, 1972, pp. 95–98.

[2]Aihara, T., "Air Cooling Techniques by Natural Convection," *Cooling Techniques for Computers*, Hemisphere, New York, 1991, pp. 1–45.

[3]Yovanovich, M. M., "New Nusselt and Sherwood Numbers for Arbitrary Isopotential Bodies at Near Zero Peclet and Rayleigh Numbers," AIAA Paper 87-1643, June 1987.

[4]Yovanovich, M. M., "Natural Convection from Isothermal Spheroids in the Conductive to Laminar Flow Regimes," AIAA Paper 87-1587, June 1987.

[5]Yovanovich, M. M., "On the Effect of Shape, Aspect Ratio and Orientation Upon Natural Convection from Isothermal Bodies of Complex Shapes," American Society of Mechanical Engineers National Heat Transfer Conf., Pittsburgh, PA, Aug. 1988.

[6]Yovanovich, M. M., Burde, S. S., and Thompson, J. C., "Thermal Constriction Resistance of Arbitrary Contacts with Constant Flux," *Thermophysics of Spacecraft and Outer Planet Entry Probes*, edited by A. M. Smith, Vol. 56, Progress in Astronautics and Aeronautics, AIAA, New York, 1977, pp. 127–139.

[7]Yovanovich, M. M., and Schneider, G. E., "Thermal Constriction Resistance Due to a Circular Annular Contact," *Thermophysics of Spacecraft and Outer Planet Entry Probes*, edited by A. M. Smith, Vol. 56, Progress in Astronautics and Aeronautics, AIAA, New York, 1977, pp. 141–154.

[8]Yovanovich, M. M., and Burde, S. S., "Centroidal and Area Average Resistances of Nonsymmetric, Singly-Connected Contacts," *AIAA Journal*, Vol. 15, No. 10, 1977, pp. 1523–1525.

[9]Yovanovich, M. M., "A General Expression for Predicting Conduction Shape Factors," *Thermophysics and Spacecraft Control*, edited by R. G. Hering, Vol. 35, MIT Press, Cambridge, MA, 1974, pp. 265–291.

[10]Chow, Y. L., and Yovanovich, M. M., "The Shape Factor of the Capacitance of a Conductor," *Journal of Applied Physics*, Vol. 53, No. 12, 1982, pp. 8470–8475.

[11]Yovanovich, M. M., and Wang, C. S., "Surface Element Method Based on Ring Sources for Accurate Calculations of Shape Factors of Complex Axisymmetric Bodies," AIAA Paper 92-2938, July 1992.

[12]Churchill, S. W., and Churchill, R. U., "A Comprehensive Correlating Equation for Heat and Component Transfer by Free Convection," *Journal of the American Institute of Chemical Engineers*, Vol. 21, No. 3, 1975, pp. 604–606.

[13]Lee, S., Yovanovich, M. M., and Jafarpur, K., "Effects of Geometry and Orientation on Laminar Natural Convection from Isothermal Bodies," *Journal of Thermophysics and Heat Transfer*, Vol. 5, No. 2, 1991, pp. 208–216.

[14]Jafarpur, K., "Analytical and Experimental Study of Laminar Free Convection Heat Transfer From Isothermal Convex Bodies of Arbitrary Shape," Ph.D. Dissertation, Dept. of Mechanical Engineering, Univ. of Waterloo, Waterloo, ON, Canada, 1992.

[15]Yovanovich, M. M., and Jafarpur, K., "Bounds on Laminar Natural Convection from Isothermal Disks and Finite Plates of Arbitrary Shape for All Orientations and Prandtl Numbers," American Society of Mechanical Engineers Winter Annual Meeting, New Orleans, LA, Nov. 1993.

[16]Bouwkamp, C. J., "A Simple Method of Calculating Electrostatic Capacity," *Physica XXIV*, Zernike Issue, 1958, pp. 538–542.

[17]Loh, S. C., "The Calculation of Electric Potential and the Capacity of a Tore by Means of Toroidal Functions," *Canadian Journal of Physics*, Vol. 37, No. 6, 1959, pp. 698–702.

[18]Loh, S. C., "On Toroidal Functions," *Canadian Journal of Physics*, Vol. 37, No. 5, 1959, pp. 619–635.

[19]Smith, T., Schneider, G. E., and Yovanovich, M. M., "Numerical Study of Conduction Heat Transfer from Toroidal Surfaces into an Infinite Domain," AIAA Paper 92-2941, July 1992.

[20]Wolfram, S., *Mathematica, A System for Doing Mathematics by Computer, Version 2 for DOS*, 2nd ed., Addison–Wesley, Reading, MA, 1992.

[21]Abramowitz, M., and Stegun, A., *Handbook of Mathematical Functions*, Dover, New York, 1970.

[22]Wang, C. S., "Surface Element Methods Based on Ring Sources and Line Sources for Accurate Calculations of Shape Factors for Arbitrary Isothermal Axisymmetric Surfaces and Some Two Dimensional Problems," M.S. Thesis, Dept. of Mechanical Engineering, Univ. of Waterloo, Waterloo, ON, Canada, 1993.

[23]McQuillan, F. J., Culham, J. R., and Yovanovich, M. M., "Properties of Dry Air as One Atmosphere," Microelectronics Heat Transfer Lab., Rept. UW/MHTL 8406 G-01, Univ. of Waterloo, Waterloo, ON, Canada, 1984.

[24]Hilsenrath, J., Beckett, C. W., and Benedict, W. S., *Tables of Thermal Properties of Matter*, National Bureau of Standards, Plenum, New York, 1970.

[25]Clemes, S. B., "Free Convection Heat Transfer from Two-Dimensional Bodies," M.S. Thesis, Dept. of Mechanical Engineering, Univ. of Waterloo, Waterloo, ON, Canada, 1990.